

Sex-Specific Pattern Formation During Early *Drosophila* Development

Manu,^{*1} Michael Z. Ludwig,^{*†1} and Martin Kreitman^{*†2}

^{*}Department of Ecology and Evolution and [†]Institute for Genomics and Systems Biology, University of Chicago, Illinois 60637

ABSTRACT The deleterious effects of different X-chromosome dosage in males and females are buffered by a process called dosage compensation, which in *Drosophila* is achieved through a doubling of X-linked transcription in males. The male-specific lethal complex mediates this process, but is known to act only after gastrulation. Recent work has shown that the transcription of X-linked genes is also upregulated in males prior to gastrulation; whether it results in functional dosage compensation is not known. Absent or partial early dosage compensation raises the possibility of sex-biased expression of key developmental genes, such as the segmentation genes controlling anteroposterior patterning. We assess the functional output of early dosage compensation by measuring the expression of *even-skipped* (*eve*) with high spatiotemporal resolution in male and female embryos. We show that *eve* has a sexually dimorphic pattern, suggesting an interaction with either X-chromosome dose or the sex determination system. By manipulating the gene copy number of an X-linked transcription factor, *giant* (*gt*), we traced sex-biased *eve* patterning to *gt* dose, indicating that early dosage compensation is functionally incomplete. Despite sex-biased *eve* expression, the gene networks downstream of *eve* are able to produce sex-independent segmentation, a point that we establish by measuring the proportions of segments in elongated germ-band embryos. Finally, we use a whole-locus *eve* transgene with modified *cis* regulation to demonstrate that segment proportions have a sex-dependent sensitivity to subtle changes in *Eve* expression. The sex independence of downstream segmentation despite this sensitivity to *Eve* expression implies that additional autosomal gene- or pathway-specific mechanisms are required to ameliorate the effects of partial early dosage compensation.

In *Drosophila*, dosage compensation occurs by an upregulation of transcription from the X chromosome in males (Mukherjee and Beermann 1965; Belote and Lucchesi 1980; Straub *et al.* 2005). The best-characterized mechanism of upregulation depends on the male-specific activity of the *male-specific lethal* (MSL) complex (Gelbart and Kuroda 2009), which binds to sites on the X chromosome and enhances the rate of transcript elongation (Larschan *et al.* 2011). MSL activity is inhibited in females by the translational repression of Msl2 protein, which is necessary for complex formation, by the protein product of the sex-determination gene *Sex-lethal* (*Sxl*) (Kelley *et al.* 1995). The canonical MSL-dependent mechanism does not appear to be active prior to gastrulation as *msl2* transcript is not detected until cleavage cycle 14

(Lott *et al.* 2011) and the earliest expression of Msl3 protein in male embryos is detected only at stage 6 (gastrulation) (Rastelli *et al.* 1995; Franke *et al.* 1996; Cline 2005).

Despite the lack of MSL-dependent dosage compensation during the blastoderm stage, the transcription of X-linked genes expressed before gastrulation is, in fact, elevated in males (Lott *et al.* 2011). With the exception of *runt* (*run*), which is known to be dosage-compensated in an MSL-independent but *Sxl*-dependent manner (Gergen 1987), the mechanism of the upregulation or dosage compensation of early expressed genes is not known.

Although the increased transcription of early expressed X-linked genes in males is suggestive of early dosage compensation, it has not yet been determined whether the observed upregulation results in functional dosage compensation. Two aspects of the pattern of upregulation of X-linked genes lead us to suspect that early dosage compensation can be incomplete: first, the pattern of upregulation is not uniform over the X chromosome, and many genes are upregulated less than twofold in males. Lott *et al.* (2011) found that 36 of 85 zygotically expressed X-linked genes had

Copyright © 2013 by the Genetics Society of America
doi: 10.1534/genetics.112.148205

Manuscript received November 30, 2012; accepted for publication February 8, 2013
Supporting information is available online at www.genetics.org/lookup/suppl/doi:10.1534/genetics.112.148205/-/DC1.

¹These authors contributed equally to this work.

²Corresponding author: Department of Ecology and Evolution, University of Chicago, 1101 E. 57th St., Chicago IL 60637-1573. E-mail: martinkreitman@gmail.com

an average female/male ratio >1.5 and that X-linked gene expression was female biased. In general, the sex ratios of gene expression were smoothly distributed between 1 and 2, similar to later, MSL-mediated compensation. The second aspect of the pattern of upregulation suggesting incomplete compensation is that the female/male ratio of transcript abundance of X-linked genes varies over cycle 14 (Lott *et al.* 2011), implying that the efficacy of early dosage compensation can also vary in time during early development.

Many early expressed X-linked genes are transcriptional regulators of key developmental processes such as anteroposterior (AP) (e.g., *giant*) and dorsoventral (e.g., *brinker*) patterning. Autosomal targets of these X-linked regulators, such as *even-skipped* (*eve*), are expressed as early as cycle 8 (Pritchard and Schubiger 1996), making it possible to test whether early dosage compensation is functional by comparing the expression of target genes in the two sexes. If the observed upregulation of the early expression of X-linked genes is still insufficient for functional dosage compensation, their autosomal targets are expected to be expressed in sexually dimorphic patterns.

We investigate the possibility of incomplete functional dosage compensation and sex-biased pattern formation by characterizing the spatiotemporal expression of an autosomal AP patterning gene (Akam 1987; Surkova *et al.* 2008), *eve*, in male and female embryos. Pattern formation has been extensively studied in *Drosophila*, but no attempt has been made in previous studies to distinguish between the two sexes. Investigations of dosage compensation (Hamada *et al.* 2005; Lott *et al.* 2011), in contrast, have ignored potential spatial and/or temporal variation in sex-biased gene expression. *eve* is expressed in seven stripes during the latter half of cleavage cycle 14 of the *Drosophila* blastoderm (Macdonald *et al.* 1986; Frasch *et al.* 1987) (Figure 1A). Each stripe is about three to five nuclei wide and is established by localized repression of early broad *eve* expression over a period of ~ 30 min (Surkova *et al.* 2008; Ludwig *et al.* 2011). Eve expression levels can be measured to an accuracy of $\sim 10\%$ (Surkova *et al.* 2008; Ludwig *et al.* 2011) and provide a sensitive readout of potential sex differences over time and position. This level of precision is desirable since the magnitude of sex ratio variation of X-linked gene expression is relatively small—at most twofold. Here we demonstrate that Eve is expressed at different levels in male and female embryos in the region between stripes one and two (1–2 interstripe).

One advantage of querying functional dosage compensation with a segmentation gene is that it is relatively easy to trace any observed difference both upstream and downstream in the well-established regulatory network (Schroeder *et al.* 2004; Jaeger 2011). It is known that the second stripe of *eve*, for example, is activated by Bicoid (Bcd) and Hunchback (Hb) and repressed in the anterior by Giant (Gt) and in the posterior by Krüppel (Kr) (Frasch and Levine 1987; Stanojevic *et al.* 1991; Small *et al.* 1992). We exploit this feature of the segmentation system to test the functional compensation of *gt*, an X-linked gene, by measuring the response of *eve* expression to *gt* dose.

Next, we determine whether the sex-biased expression of Eve also leads to sex-biased segmentation during later development. Eve is a regulator of the segment-polarity gene *engrailed* (*en*) (Macdonald *et al.* 1986; Fujioka *et al.* 1995; Fujioka *et al.* 2002), which, along with *wingless* (*wg*), establishes the molecular prepatterning of the segmented embryo (Ingham *et al.* 1985; Baker 1987). *en* patterning and the proportions of parasegments have not yet been critically examined in the sexes. Using En expression as a marker, we measure the ratio of parasegments in extended germ-band embryos of each sex to establish that segmentation at a later developmental stage is sex-independent.

A potential explanation for the robustness of *en* patterning and parasegment proportions is that *en* expression is insensitive to Eve expression in the 1–2 interstripe region. In a final set of experiments, we test this hypothesis by characterizing the sensitivity of *en* expression to Eve expression in the 1–2 interstripe. For this purpose, we take advantage of an *eve* transgene that has a reduced level of Eve expression in the interstripe region. This transgene was derived from the endogenous *eve* locus by modifying the *cis* regulation of the stripe 2 enhancer (S2E) (Ludwig *et al.* 2011). S2E is ~ 800 bp long and contains 17 binding sites, identified by *in vitro* DNase protection assays, for Bcd, Hb, Gt, and Kr (Figure 1B). A 480-bp fragment, called the minimal stripe 2 element, is, however, necessary and sufficient for stripe 2 expression (Small *et al.* 1992; Ludwig *et al.* 2005). The transgene MSE was derived from the endogenous locus by deleting 244 bp of sequence flanking the minimal stripe 2 element and tagging the C terminus of Eve with yellow fluorescent protein (YFP). We also constructed a control YFP-tagged transgene, “WT”, which has wild-type *eve cis*-regulatory sequences. Both WT and MSE provided healthy rescue of the lethality of *eve*^{R13}, a null allele; *Df(2R)eve*, a small deletion covering *eve*; and *eve*^{ΔMSE}, a synthetic allele of *eve* in which the minimal stripe 2 element has been replaced by *w*⁺ sequence. Nevertheless, MSE drove defective stripe 2 formation: Eve expression was lower in both stripe 2 and the 1–2 interstripe region.

We measure Eve and En expression driven by the MSE transgene in each sex to show that (1) 1–2 interstripe Eve expression is lowered specifically in males and becomes indistinguishable from the female level and (2) En expression and parasegment proportions are perturbed in males to give sex-biased segmentation in MSE. Based on these results we argue that *en* regulation is sensitive to the level of Eve expression in the 1–2 interstripe and postulate that additional mechanisms must act on the segmentation genes to ensure sex-independent larval segmentation in the wild type.

Materials and Methods

Stocks and transgenic fly lines

The following laboratory stocks were used: *w*¹¹¹⁸, *y*¹, *sc*¹, *gt*^{X11}/FM6 (Bloomington 1529) and *Df(1)JA27/FM7c,P*

[*GAL4-Kr.C*],*P*[*UAS-GFP.S65T*] (Bloomington 5193). The latter two stocks were crossed to produce $y^1,sc^1,gt^{X11}/FM7c,P[GAL4-Kr.C],P[UAS-GFP.S65T]$ flies. *eve*^{ΔMSE} is a recessive lethal mutant of *eve* created by replacing the 480-bp fragment corresponding to the minimal stripe 2 element from the endogenous *eve* locus with the *white*+ gene using ends-out homologous recombination (Ludwig *et al.* 2011).

The construction of the transgenic strains is reported in detail elsewhere (Ludwig *et al.* 2011). Briefly, WT is a 16.4-kb fragment from the *eve* locus created by recombineering with a Red/ET counterselection BAC Modification Kit (Gene Bridges GmbH, Heidelberg, Germany). A superfolding variant of YFP, SYFP2 (Ben Glick, University of Chicago), was added to the C terminus of the Eve peptide, allowing us to visualize transgenic expression independently of the endogenous locus. MSE was derived from WT by deleting 33 and 211 bp 5' and 3' of the minimal stripe 2 element, respectively (Figure 2A). Both constructs were integrated into the same site on the third chromosome (*attP2*) using *phiC31* site-specific integration (Markstein *et al.* 2008). The *gt*^{YFP} construct was made similarly, using a 26.2-kb region of the *gt* locus, tagged with SYFP2 employing *Drosophila* codon usage (Supporting Information, File S1), and provides healthy rescue of a null allele of *gt*, *gt*^{X11} (Table S2).

Genetic crosses, staining, and genotyping for En and Eve patterning

Wild-type Eve patterning was assayed in *w*¹¹¹⁸ embryos (Figure 1). Eve patterning driven by the WT and MSE transgenes (Figure 2) was assayed in embryos from a cross between *eve*^{R13}/*CyO*,*P*[*hb-LacZ*] females and *eve*^{R13};WT(MSE) males, yielding the *eve*^{R13};WT(MSE)/+ or *eve*^{R13}/*CyO*,*P*[*hb-LacZ*];WT(MSE)/+ genotypes. The *gt* dosage series (Figure 3) was constructed in two separate crosses. Genotypes with zero to two doses were the offspring of a cross between *gt*^{X11}/*FM7c*,*P*[*GAL4-Kr.C*],*P*[*UAS-GFP.S65T*] females and *w*¹¹¹⁸ (*w*⁻) males while the three- to four-dose genotypes were the offspring of the cross between *gt*^{YFP} males and females. To measure the effects of the rescue transgenes on En pattern and segmentation (Figure 4), we crossed *eve*^{ΔMSE}/*CyO*,*P*[*hb-LacZ*] and *eve*^{R13};WT(MSE) flies and collected embryos for further analysis.

Embryos were collected, fixed, and immunostained with antibodies against Eve (Figures 1E and 3), GFP (Figure 2), or En (Figure 4) as described (Ludwig *et al.* 2005, 2011). Embryos stained fluorescently for GFP and Eve were imaged with a confocal microscope (see below). The lengths of both parasegments 3 and 4 in En pattern were measured at the ventral site of early stage 11 embryos. The reported numbers are the mean of three repeated measurements by hand using ImageJ (National Institutes of Health). After imaging, individual embryos were genotyped by PCR with primers for the Y chromosome, *P*[*hb-LacZ*], and *P*[*UAS-GFP.S65T*] (File S1) to determine sex and *eve* or *gt* dosage. The protocol is available on request.

Confocal imaging and feature detection

Immunofluorescently stained embryos were imaged with a Vti Infinity 3 confocal (Visitech International, Sunderland, MA) and a Zeiss AxioPlan 2 microscope (Carl Zeiss, Inc.) using a 16× PLAN-NEOFLUAR objective. The 491-, 561-, 642-nm lasers, a 488/565/643 dichroic, 535/605/700 emission filter, and an EMCCD camera (Hamamatsu Photonics UK Ltd., Hertfordshire, UK) were employed to acquire images at a resolution of 512 × 512. To maximize dynamic range, camera gain and exposure were chosen so that the brightest embryos in an experiment had a few saturated pixels. All the embryos in an experiment, irrespective of genotype, were imaged with the same settings. Laterally oriented embryos were imaged in three planes 1 μm apart transecting the nuclei at the embryo surface flattened against the coverslip, and the images were averaged. Embryos were also imaged at the mid-sagittal plane to determine their length.

Embryos were staged according to a standard scheme (Surkova *et al.* 2008) using only membrane invagination as a marker; “early” cycle 14 corresponds to time classes T3–T4, the earliest time at which a nascent stripe 2 is detectable; “middle” is T5–T6; and “late” is T7–T8, ~9 min prior to gastrulation. The images were segmented using described methods (Janssens *et al.* 2005), and the location of and the mean fluorescence intensity in each nucleus were saved for further processing.

The positions of and expression values at the extrema were estimated using a smoothing cubic spline (CSAPS function of MATLAB, MathWorks Inc.) fit to data extracted from the nuclei lying in a 10%-wide dorsoventral strip along the anteroposterior axis. The level of smoothing was chosen to minimize the error made by the spline approximation without detecting spurious extrema (Ludwig *et al.* 2011). The same level of smoothing was applied to all embryos in the same time class irrespective of experiment or genotype. The error made by the spline approximation at the extrema was ~5%.

Results

Sex-specific eve expression in wild type

To investigate early dosage compensation, we measured the spatiotemporal dynamics of *eve* expression separately in male and female embryos. We fluorescently immunostained embryos of a standard laboratory stock, *w*¹¹¹⁸, with anti-Eve antibody. These embryos were mounted one per slide and imaged with a confocal microscope. After imaging, the embryo was removed and genotyped for sex using PCR. The images were staged into three classes according to the scheme of Surkova *et al.* (2008), using only nuclear morphology and membrane invagination as markers. Each class is ~12 min long, spanning the period from early cycle 14 when Eve is expressed in a triband pattern, to just before gastrulation, when Eve is expressed in seven fully mature

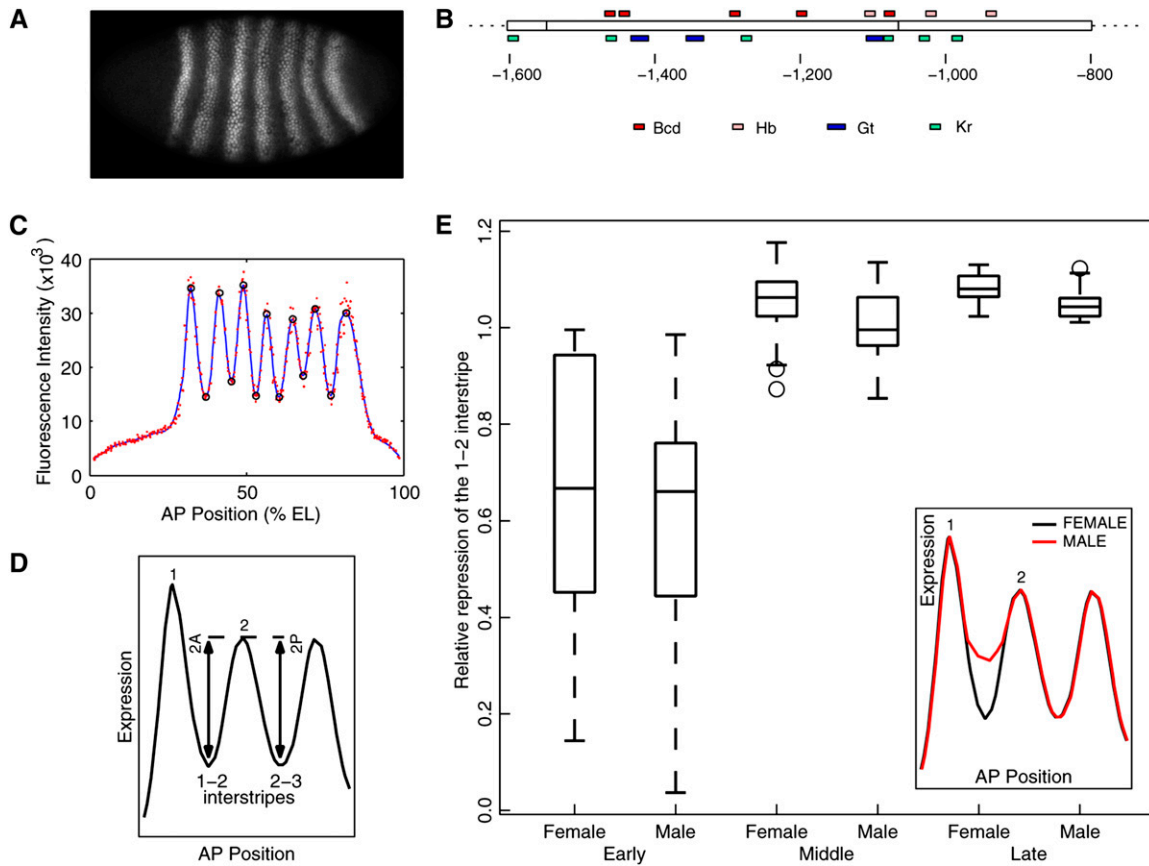


Figure 1 Sexually dimorphic Eve expression in w^{1118} . (A) The Eve expression pattern in middle–late cleavage cycle 14. Anterior is to the left and dorsal is above. (B) The 800-bp-long 5' regulatory region that drives stripe 2 expression (Ludwig *et al.* 2005). Distance is relative to the transcription start site. The box in the middle is the minimal stripe 2 element. Footprinted binding sites (Stanojevic *et al.* 1989; Small *et al.* 1991) for the activators Bicoid (Bcd) and Hunchback (Hb) and for the repressors Giant (Gt) and Krüppel (Kr) are shown above and below, respectively. (C) Measurement of the features of the Eve expression pattern. The red points are average fluorescence intensities of Eve staining in nuclei lying in a strip that extends 10% dorsoventrally around the AP axis. The blue line is a smoothing cubic spline fit to data. Black circles are local maxima and minima of the spline. (D) Schematic of the measurement of stripe 2 border height. (E) Boxplot of relative repression of the 1–2 interstripe in w^{1118} embryos. In all boxplots shown, the box lines are the first quartile, median, and the third quartile. The whiskers extend to the most extreme values lying within 1.5 times the interquartile range, and any datapoints outside the whiskers are shown as circles. Embryos were classified into three 12-min long bins: early, middle, and late (see *Materials and Methods*). Relative repression was measured as the ratio of the height of the anterior border to that of the posterior border (D). $n = 14, 13, 25, 31, 16, 15$. The inset is a schematic illustration of the sex-specific expression of Eve.

saw-tooth-shaped stripes (Frasch *et al.* 1987; Surkova *et al.* 2008). We processed the confocal images using an image-processing algorithm (Janssens *et al.* 2005) to estimate Eve expression in individual nuclei. Finally, we extracted data from a narrow strip lying along the AP axis of the embryo and fit a cubic spline to these data to measure several features of the pattern (Figure 1C).

In all, we measured 43 features of the Eve pattern. We estimated the expression level at the peak of each stripe and at the trough between two stripe peaks, henceforth referred to as the “interstripe.” These measurements were normalized to the mean of Eve expression in all nuclei of the embryo to correct for experimental image intensity variation. We also computed the positions of the stripe peaks, interstripe troughs, and the stripe borders along the AP axis. Since Eve stripes form by localized repression in the interstripe nuclei (Stanojevic *et al.* 1991; Small *et al.* 1992), we also define a measure for

the strength of repression in an interstripe. Let the height of a stripe border be the difference in the expression level of the stripe peak and the interstripe trough (for example, 2A in Figure 1D). We take the ratio of the border heights of the two borders of a stripe, for example, 2A and 2P in Figure 1D, to obtain a normalized measure of the repression of a border, which we refer to as “relative repression.”

We found evidence for sex-specific patterning differences in the relative repression of three of the seven Eve stripes: stripe 2 (Figure 1E; $P = 0.0538$ mid-cycle 14 and $P = 0.0096$ late cycle 14; the Wilcoxon rank-sum test was used here and in all subsequent statistical tests), stripe 3 (Figure S1C, $P = 0.0312$ late cycle 14), and stripe 4 (Figure S1C, $P = 0.0345$ late cycle 14). No sex bias was detectable in any of the other features (Figure S1 and Figure S2).

As we show below, the relative repression of stripe 2 (Figure 1E) is the most consistent sex-biased patterning

feature, and we focused our subsequent analysis on this feature. There is no detectable difference in early cycle 14, possibly due to the large variability of relative repression during the early stages of stripe 2 formation (Ludwig *et al.* 2011) (Figure 1E). A measurable difference of $\sim 7\%$ appears in middle cycle 14 (Figure 1E), with the male having a lower value of relative repression than the female. The difference reduces to $\sim 4\%$ in late cycle 14, but is still statistically significant due to the precise measurement allowed by the low variability of the late Eve pattern; the standard deviation of relative repression is $\sim 3\%$.

Lower values of relative repression imply that the male embryo has a shorter—that is, derepressed—stripe 2 anterior border compared to the female, which is shown schematically in the inset of Figure 1E. We could detect greater Eve expression in the 1–2 interstripe in males during late cycle 14 (Figure S3A, $P = 0.0604$), whereas no sex difference was detectable in Eve expression in the 2–3 interstripe (Figure S3B, $P > 0.2$), suggesting that sex-biased relative repression is attributable to higher Eve expression in the 1–2 interstripe.

Sex-specific features of Eve patterning were rechecked in independent experiments using the WT *eve* transgene, a 16.4-kb region from the *eve* locus, tagged with YFP and integrated on the third chromosome (Table S1). We crossed *eve^{R13}/CyO,P[hb-Lacz]* females with *eve^{R13};WT* males. Embryos collected from the cross were mounted, imaged, and genotyped in the same manner as the *w¹¹¹⁸* embryos, with two differences. First, we detected the CyO balancer by co-staining with β -galactosidase antibody to identify embryos with one (*eve^{R13};WT/+*) or two (*eve^{R13}/CyO,P[hb-Lacz];WT/+*) *eve* doses. Second, we focused on middle cycle 14 to maximize sample size since this cross produced many more genotypes than the *w¹¹¹⁸* experiment.

This experiment confirmed the sex-dependent patterning of stripe 2. Males have a derepressed anterior border compared to females in WT (Figure 2B; $P = 0.0012$, one *eve* dose and $P = 0.0346$, two *eve* doses). Relative repression and 1–2 interstripe expression were the only sex-biased stripe 2 features in WT (Figure S4); Eve expression in the 1–2 interstripe was elevated in males relative to females (Figure S5; $P = 0.0021$, one *eve* dose and $P = 0.2395$, two *eve* doses), replicating *w¹¹¹⁸* results. The derepression of the 1–2 interstripe is *eve*-dose-dependent since relative repression differs between the sexes by ~ 22 and $\sim 8\%$ in the one- and two-dose rescues, respectively (Figure 2B). The other sex differences—in the relative repression of stripes 3 and 4 in *w¹¹¹⁸* (Figure S1C) and a new one found in this experiment in the relative repression of stripe 5 (Figure S6C)—were inconsistent between the two experiments.

Incomplete dosage compensation of *gt*

The sex-specific features of *eve* expression in wild type implies that there is an as-yet-unappreciated interaction between the sex determination or dosage compensation systems and the segmentation genes. One possibility is that sex-

determination genes, such as *Sxl*, regulate *eve*'s expression in the 1–2 interstripe. Another possibility is that one or more X-linked genes regulating *eve* are not dosage-compensated and have different levels of expression in the two sexes, resulting in *eve*'s sex-dependent features. To regulate *eve* specifically in the 1–2 interstripe, the sex-determination genes would need to be expressed in an AP-position-dependent manner, but are, in fact, expressed uniformly throughout the embryo (Erickson and Cline 1993). Although uniform expression does not completely preclude an interaction with *eve*, we first checked the latter possibility—that *eve*'s sex-specific expression originates in the lack of dosage compensation for one or more X-linked loci—by varying the dosage of a candidate X-linked locus, *gt*, and measuring the response of the *eve* interstripe phenotype.

gt is a promising candidate as a source of dimorphic *eve* expression in the 1–2 interstripe because Gt protein is known to repress *eve* expression in that region. The minimal stripe 2 enhancer contains three footprinted binding sites for Gt (Stanojevic *et al.* 1991; Small *et al.* 1992). Deletion of these sites leads to a derepression of the anterior border in a reporter assay (Stanojevic *et al.* 1991; Small *et al.* 1992). Stripes 1 and 2 are fused in *gt⁻* embryos (Frasch *et al.* 1987), suggesting that the phenotype is responsive to *gt* dose. Given the known role of Gt as a repressor of *eve*, the observed derepression of *eve* expression in the 1–2 interstripe is consistent with a lower level of Gt protein expression in male embryos.

Our strategy was to vary the gene dose of *gt* in the two sexes and to measure the response of the *eve* 1–2 interstripe phenotype. The reasons to measure the response of *eve* instead of Gt expression levels directly are twofold. First, the difference between male and female *gt* expression is potentially quite small (Lott *et al.* 2011), and the precise and dynamic spatiotemporal expression of *eve* allows for much greater sensitivity of detection. Second, this experiment would test not only whether *gt* is dosage-compensated but also whether it drives the observed sex-specific features of *eve* expression.

We crossed *gt^{X11}/FM7c* flies (a null allele; Table S1) to *w¹¹¹⁸* to generate *gt⁻* male embryos (0M; the number is *gt* dose and the letter signifies sex), 1-*gt*-dose female embryos (1F), 1-*gt*-dose male embryos (1M), and 2-*gt*-dose female embryos (2F) (Figure 3A). Using the same experimental procedures used to establish the sex-specific expression of Eve, we imaged Eve expression and measured its features quantitatively in these genotypes. In agreement with our earlier results, the 1M genotype has a derepressed 1–2 interstripe relative to 2F in middle cycle 14 (Figure 3B, $P = 0.0011$).

The 1F genotype is hemizygous for *gt* but homozygous for all other X-linked loci. 1F also produces a derepressed interstripe (Figure 3B, $P = 0.0002$), showing that a lower *gt* dose leads to a derepression of the 1–2 interstripe in female embryos. In fact, 1F and 1M are indistinguishable from each other ($P = 0.3864$), strongly suggesting that *gt* accounts for all of the effect.

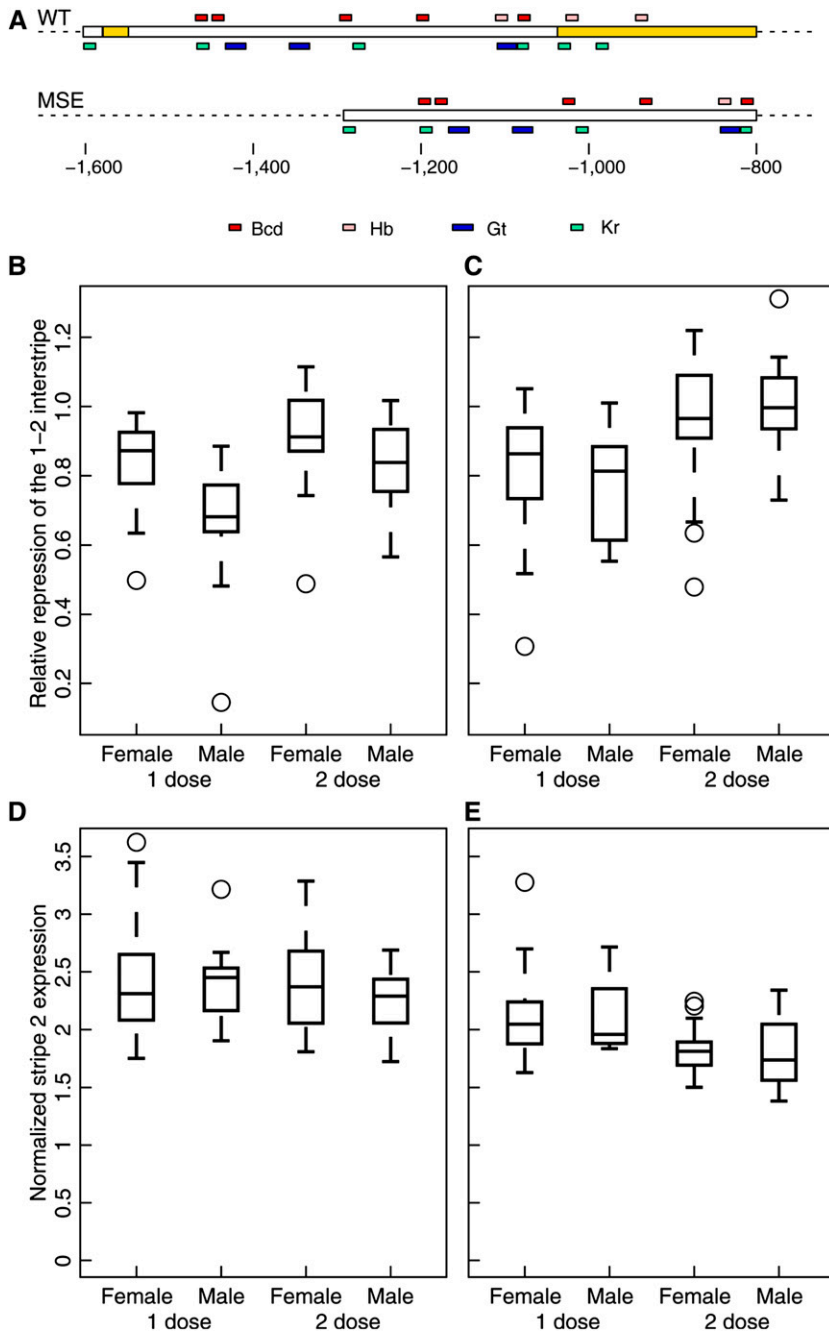


Figure 2 Stripe 2 expression is sexually dimorphic in WT but lacks sex bias in MSE. Embryos had one copy of the transgene and were either null (*eve^{R13};WT(MSE)/+*) or hemizygous (*eve^{R13}/CyO,P[hb-LacZ];WT(MSE)/+*) for endogenous *eve*, giving a total *eve* dose of either one or two, respectively. Data are from embryos in mid-cycle 14 stained for Eve-YFP with anti-GFP. (A) The stripe 2 regulatory region in the WT and MSE *eve* transgenes. Yellow regions were deleted in MSE. Binding sites are shown as in Figure 1B. (B and D) WT. (C and E) MSE. (B and C) Boxplots of relative repression of the 1–2 interstripe. Relative repression was measured as the ratio of the height of the anterior border to that of the posterior border (Figure 1D). (B) WT; $n = 20, 15, 18, 20$. (C) MSE; $n = 25, 20, 23, 9$. (D and E) Boxplots of expression at stripe 2 peak. Peak expression was normalized to mean Eve fluorescence in each embryo. Sample sizes are the same as in B and C.

Because *gt* regulates the expression of *eve* 5–6 and 6–7 interstripes (Frasch and Levine 1987) in addition to that of interstripe 1–2, their expression should have a similar response to *gt* dose. Figure S7 shows the *P*-values of the rank-sum test for relative interstripe expression between 2F and 0M, 1F, or 1M. 0M (*gt⁻*) differs from 2F in the interstripes 1–2, 5–6, and 6–7. Both 1M and 1F differ from 2F in the 1–2 and 6–7 interstripes but not elsewhere.

We also used a whole-locus transgene for *gt*, *gt-YFP* (Table S1), which provides healthy rescue of *gt⁻* (Table S2) to boost *gt* dose to 3 in males (3M) and 4 in females (4F) (Figure 3A). As expected, repression of the 1–2 interstripe is an increasing function of *gt* dose (Figure 3B). The dose-

response curve saturates after two doses, however, suggesting that two *gt* doses are sufficient to completely turn off *eve* transcription in 1–2 interstripe nuclei.

Late segmentation is sex-independent

Do the sex-dependent features of Eve expression lead to sexually dimorphic segmentation of the embryo? Although no gross differences in the segmentation of embryos between males and females have been observed to date, we conducted a quantitative analysis to detect more subtle differences in the proportions of segments. We measured the proportions of parasegments 3 and 4 in extended germ-band-stage embryos using En expression as a marker. *en* is

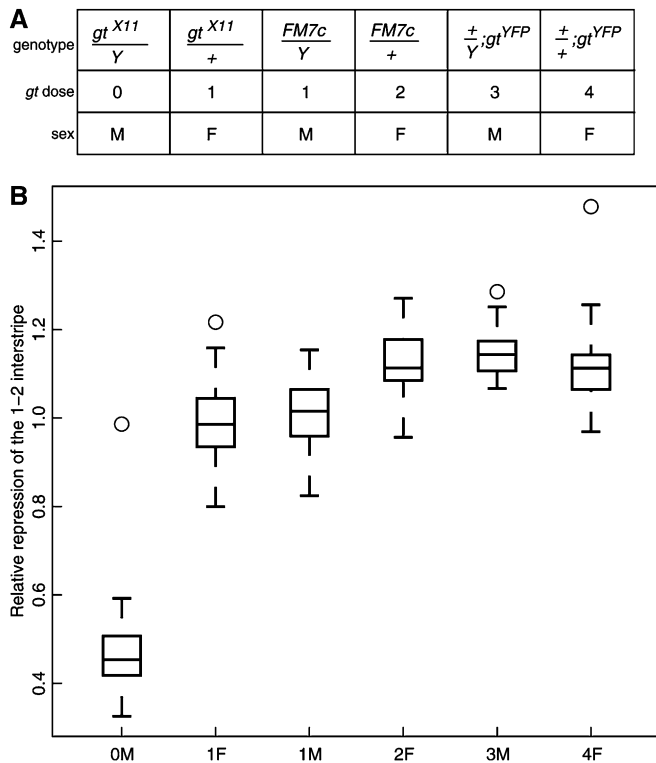


Figure 3 The response of stripe 2 relative repression to *gt* dose. (A) The genotypes used to make a dosage series for *gt*. (B) Response of the relative repression of the 1–2 interstripe to *gt* dose. Relative repression was measured as before (Figure 1, D and E). Embryos were at mid-cycle 14. $n = 13, 28, 16, 14, 22, 17$.

expressed in the anterior part of parasegments, and its anterior margin marks parasegmental grooves (Ingham *et al.* 1985). Parasegment 3 is under the control of Eve expression in stripe 2 since embryos homozygous for *eve* ^{Δ MSE} (Table S1), the endogenous *eve* locus in which the stripe 2 enhancer has been replaced by *w*⁺ sequence, lack *eve* stripe 2 expression and have defective third parasegments (Ludwig *et al.* 2005).

We crossed *eve* ^{Δ MSE}/*CyO*,*P*[*hb-LacZ*] and *eve*^{R13}/*WT* flies to specifically rescue the lethality of stripe 2 ablation with one dose of the WT *eve* transgene. Stage 11 embryos were costained with β -galactosidase to identify the *eve* ^{Δ MSE}/*eve*^{R13} genotype and En antibodies. We measured the number of pixels between the anterior margins of En stripes 3–4 and 4–5 on the ventral side to estimate of the length of parasegments 3 and 4, respectively (Figure 4A). The length of parasegment 3 was normalized to that of the total length of parasegments 3 and 4 to correct for variation in embryo size. This comparison between male and female embryos revealed no evidence for a difference in the median ratio of the parasegmental length of 3 to 3 + 4 (Figure 4B, $P = 0.2937$). The sex-specific features of Eve stripe 2 expression do not, therefore, appear to be carried forward developmentally to segmentation in extended germ-band-stage embryos.

Sex-independent segmentation in WT requires compensatory mechanisms

The sex-dependent features of *eve* expression pose potential challenges for its downstream targets, such as the pair-rule genes *fushi-tarazu*, *run*t, and *hairy* and the segment polarity genes *en* and *wg*. For late segmentation to be the same in the two sexes, are downstream genes indifferent to sex-specific *eve* expression? Or are there mechanisms interceding to attenuate the sex-dependent differences in *eve* expression?

The relative repression in males differs by a small amount, $\sim 10\%$, from the female level. One possible explanation for the apparent robustness is simply that *en* or other *eve* targets are insensitive to the relative repression of stripe 2. In this section, we test the sensitivity of *en* regulation to sex-specific Eve expression by assaying Eve and En expression in male and female embryos of a transgenic line having altered levels of relative repression.

In earlier work investigating the robustness of the *cis* regulation of *eve* stripe 2 (Ludwig *et al.* 2011), we modified the WT *eve* transgene to create another transgene, MSE (Table S1). MSE was derived from the WT transgene by deleting 244 bp of regulatory sequence flanking the minimal stripe 2 element (Figure 2A). Stripe 2 expression driven by the MSE transgene is weaker than WT expression, has greater variability than WT, and lacks temperature compensation.

Of more direct interest to us, MSE also has a different level of interstripe repression than WT, which offers an opportunity to test the potential functional impact of interstripe derepression in males. Time series data of live Eve-YFP expression showed that the relative repression of the 1–2 interstripe was greater in MSE relative to WT (Ludwig *et al.* 2011). If the $\sim 10\%$ difference between males and females is functionally relevant, modulation of the level of repression should result in downstream segmentation phenotypes.

The live-imaging experiments (Ludwig *et al.* 2011) had not distinguished between the sexes; male or female embryos, or both, might have greater relative repression than their WT counterparts. We therefore measured the features of Eve expression driven by the MSE transgene separately in fixed male and female embryos that had either one (*eve*^{R13}/*MSE*/+) or two (*eve*^{R13}/*CyO*,*P*[*hb-LacZ*];*MSE*/+) doses of *eve*. Confocal imaging and image processing of MSE were carried out with settings identical to WT.

MSE males lose the derepression of the 1–2 interstripe and have a level of relative repression indistinguishable from MSE females (Figure 2C; $P = 0.3145$, one dose, and $P = 0.5686$, two doses). The increase in relative repression in MSE relative to WT is restricted to males (Figure 2, B and C; $P = 0.3711$, one dose, and $P = 0.0002$, two doses), and relative repression is not altered in females (Figure 2, B and C; $P = 0.7609$, one dose, and $P = 0.2423$, two doses); the sequences removed in MSE appear to affect *eve* expression specifically in males. One possible explanation for the insensitivity of relative repression in females is that two *gt* copies are sufficient to completely turn transcription off in

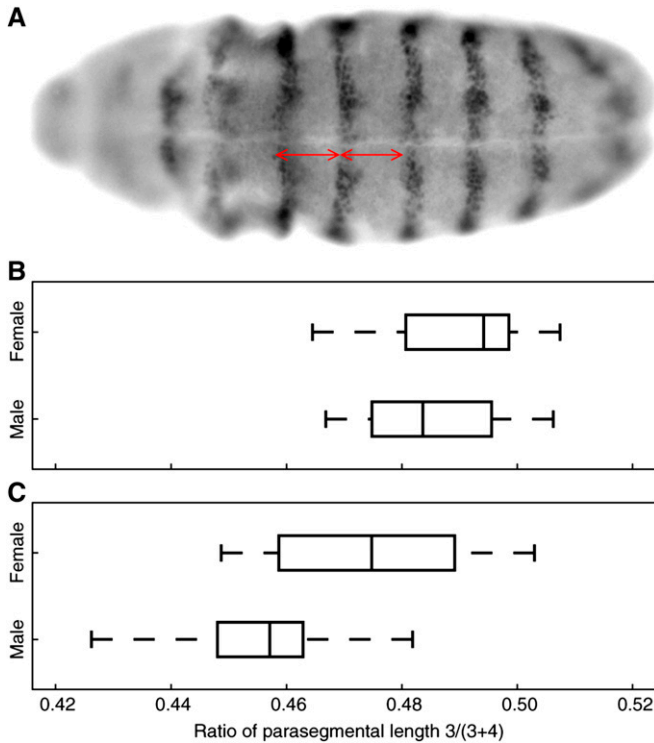


Figure 4 Parasegmental proportions in the rescue of *eve*^{ΔMSE/eve^{R13}} lethality by the WT or MSE transgenes. The genotype of the rescued embryos is *eve*^{ΔMSE/eve^{R13}}; *WT(MSE)*/. (A) Ventral view of a stage 11 embryo stained for En. Red lines show the measurement of the length of parasegments 3 (left) and 4 (right). (B and C) Boxplot of the ratio of parasegment 3 length to the total length of 3 and 4. (B) WT; from top to bottom, *n* = 8, 13 embryos. (C) MSE; *n* = 14, 7 embryos.

the interstripe (Figure 3B). We were not able to detect sex-specific expression in any other stripe 2 feature in MSE (Figure S4). In particular, although peak stripe 2 expression is lower in MSE relative to WT [Figure 2, D and E; $P(\text{female}) = 0.0126$ and $P(\text{male}) = 0.0950$ in one dose, $P(\text{female}) = 4.9548E-6$ and $P(\text{male}) = 0.0001$ in two doses], peak expression does not differ between males and females in either line ($P > 0.4$, WT, and $P > 0.6$, MSE). The loss of 1–2 interstripe derepression in MSE males allows us to test its functional impact on downstream segmentation.

We assayed the proportions of parasegments 3 and 4 in *eve*^{ΔMSE} embryos rescued by one dose of the MSE transgene in the same manner as WT. We found that *eve* misregulation by MSE induces sex-specific *en* patterning. In contrast to WT (Figure 4B), the median ratio of the parasegmental length of 3 to 3 + 4 differs significantly between MSE males and females (Figure 4C; $P = 0.0571$). Assuming that each parasegment is 20 cells long (Ingham *et al.* 1985), the difference in MSE males and females (3.7%) corresponds to a shift of about one cell. This result indicates that the proportions of parasegments 3 and 4 are sensitive to subtle alteration of Eve expression. Even though both 1–2 interstripe and peak stripe 2 expression are altered in MSE, only the former is sex-dependent (Figure 2). For this reason, we tentatively

conclude that the sex bias in *En* patterning results specifically from the sensitivity of *en* regulation to Eve 1-2 interstripe repression. It is not the case that sexually dimorphic *eve* expression is simply below the detection limit of downstream gene regulation. This in turn implies that as-yet-unknown mechanisms must compensate for sexually dimorphic *eve* expression in WT to produce sex-independent segmentation.

Discussion

Genomic transcriptional profiling of individual embryos established that transcription from the X chromosome is upregulated in males prior to gastrulation (Lott *et al.* 2011). It was not known whether the upregulation of transcription in males leads to functional dosage compensation. We suspected that early dosage compensation might be incomplete since the female/male ratio of gene expression is not uniform but rather varies between 1 (perfect compensation) and 2 (no compensation) (Lott *et al.* 2011). Incomplete early dosage compensation could lead to sex-biased pattern formation in the blastoderm.

We confirmed this suspicion by measuring the spatio-temporal expression of *eve* in wild-type male and female embryos. Whereas studies of spatiotemporally resolved patterning have ignored sex (Fowlkes *et al.* 2008; Surkova *et al.* 2008), genome-wide studies of dosage compensation (Hamada *et al.* 2005; Lott *et al.* 2011) have relied on whole-embryo extracts and hence have ignored differential spatial regulation between the two sexes. Eve expression differs between males and females in the 1–2 interstripe (Figures 1E and 2B) and perhaps in the 5–6 and 6–7 interstripes (Figure S7), which altogether comprise only ~15% of embryo length. Dimorphic patterning of *eve* is remarkable since the robustness of *eve* expression has been extensively documented (Lucchetta *et al.* 2005; Holloway *et al.* 2006; Lott *et al.* 2007; Surkova *et al.* 2008; Ludwig *et al.* 2011); this is perhaps the first example of the lack of robustness among the segmentation genes.

Genetic analysis showed that the derepression phenotype is under the specific control of *gt* dose (Figure 3B). Despite empirical evidence for the upregulation of *gt* transcription in males (Lott *et al.* 2011), our results suggest that *gt* dosage compensation is partial and that incomplete compensation has functional consequences. It is notable that 1-*gt*-dose males and females are indistinguishable with respect to 1–2 interstripe repression (Figure 3B). The equivalence of *gt* functional output in males and hemizygous females implies that the mechanism compensating for *gt* dose operates independently of sex. *run* was found to rely on Sxl for its dosage compensation (Gergen 1987), and its messenger RNA (mRNA) contains Sxl-binding sites (Kelley *et al.* 1995). Consistent with a non-sex-dependent mode of compensation, *gt* mRNA lacks Sxl-binding sites (Lott *et al.* 2011).

Despite *eve*'s sex-biased expression, we could not detect any sex bias in the expression of *En* in extended germ-band

eve^{ΔMSE/eve^{R13};WT/+} embryos (Figure 4B). It is possible that the shift in the placement of parasegments is smaller than our measurement precision. However, given that we can detect a sex-specific shift of about one cell in *eve*^{ΔMSE/eve^{R13};MSE/+} embryos, the shift in WT, if any, is likely too small to be biologically meaningful.

The differential expression of *Eve* in WT and MSE suggests two alternative hypotheses for the sex-specific shift in parasegment 3 *En* expression in MSE. Stripe 2 expression differs between WT and MSE in two aspects (Ludwig *et al.* 2011): (1) 1–2 interstripe repression is greater in MSE (Figure 2, B and C) and (2) peak expression is lower in MSE (Figure 2, D and E). According to the first hypothesis, the shift of parasegment 3 *En* expression in MSE males is specifically attributable to the first *Eve* phenotype—*i.e.*, greater repression of the 1–2 interstripe. The alternative hypothesis proposes that the shift in *En* expression is due to lowered *Eve* stripe 2 expression in MSE, whereas its sex dependence arises for unrelated and as-yet-undefined reasons. We favor the first explanation for two reasons: (1) the increased repression of the 1–2 interstripe is, in fact, a sex-dependent *Eve* phenotype (Figure 2 and Figure S4) and (2) it is unlikely that the sex dependence of the *En* phenotype is unrelated to *Eve* expression because WT and MSE are co-isogenic strains, differing only in their *eve* transgene sequence. Nevertheless, experiments selectively disrupting either 1–2 interstripe expression or peak stripe 2 expression will be required to conclusively distinguish between these two hypotheses.

We propose that additional mechanisms are required to compensate for the effects of dimorphic *Eve* expression and to produce sex-independent *En* patterning. Our results allow us to infer some general properties of such buffering. First, it must be independent of known dosage compensation mechanisms since it would have to act on autosomal gene expression in a tissue-specific manner. Second, the mechanism appears to be specifically targeted to the derepression of the 1–2 interstripe in wild-type males since the MSE line, which has lost the derepression, has defective *En* patterning. One hypothesis for a downstream buffering mechanism is *eve* autoregulation (Harding *et al.* 1989) because we observe a smaller median shift of relative repression between males and females with two *eve* doses (Figure 2B, 8%) than with one *eve* dose (22%). Alternatively, the differential expression of *gt* may induce sex-specific expression in other pair-rule genes, which in turn could compensate for sex-specific *eve* expression in the regulation of the segment polarity genes. This might explain why *en* expression becomes sex-biased (Figure 4C) when *eve* is misregulated in MSE to have sex-independent expression (Figure 2C). The MSE transgene also shows that a functional stripe 2 enhancer architecture that suppresses sex-specific *gt* expression is possible even though the WT enhancer itself transduces differential *gt* expression. *Cis*-regulatory architecture, therefore, may be playing an integral role in fine-tuning sex-biased gene expression and perhaps has evolutionarily conserved features.

In previous work (Ludwig *et al.* 2011), we noted that the modifications to *eve*'s *cis*-regulation in MSE sensitize the strain to X-dosage perturbations. Even though both WT and MSE rescue *eve*^{R13} lethality with high efficiency, the male/female ratio is much lower in rescue by MSE [$P = 0.01$, homozygote; $P = 2.3E-23$, hemizygote; figure 1B and figure S1 of Ludwig *et al.* (2011), respectively]. Sensitivity to X dosage appears to specifically originate in stripe 2 regulatory sequences: while both WT and MSE rescue the lethality of *eve*^{ΔMSE} (Ludwig *et al.* 2005, 2011), an *eve* locus lacking the minimal stripe 2 element, only the MSE rescue genotype exhibits a reduced male/female ratio [$P = 2.1E-5$; figure S3 of Ludwig *et al.* (2011)].

Based on available evidence, we argue that the modulation of the repression of the 1–2 interstripe by *gt* dosage and stripe 2 *cis*-regulatory interactions underlies the sensitivity of the MSE strain to X dosage, although a definitive proof of causality will have to await further experiments. First, the loss of adult male viability in MSE is not peculiar to any mutant chromosome; the rescue of all tested chromosomes—*eve*^{R13/eve}^{R13}, *eve*^{R13/Df(2R)eve}, and *eve*^{ΔMSE/eve}^{R13}—shows loss of male viability (Ludwig *et al.* 2011). Second, in hemizygous rescue, MSE has significantly greater lethality than WT during embryogenesis, a point established in our earlier study (Ludwig *et al.* 2011). Third, as we noted above, the loss of male viability originates specifically in stripe 2 sequences; the WT and MSE transgenes are co-isogenic except for 244 bp of sequence flanking the minimal stripe 2 element. Notwithstanding these arguments, it is possible that the mutated stripe 2 sequences cause lethality not via parasegment 3 *en* misregulation, but by their pleiotropic effects on *eve* regulation in other tissues, such as the CNS (Fujioka *et al.* 1999). Although enhancers have been regarded as largely autonomous so far, long-range interactions between enhancers have been reported recently (Dunipace *et al.* 2011; Perry *et al.* 2011). Inspecting *eve*'s neuronal expression for sex bias might help to affirm or eliminate this possibility.

The incomplete dosage compensation of *gt* induces differences that are able to propagate through the segmentation hierarchy to the pair-rule genes in a sex-specific manner, but are attenuated before reaching the segment-polarity genes. We speculate that the propagation of these differences and mechanisms for their correction must be widespread since incomplete dosage compensation itself is common in other organisms and in evolution. In *Drosophila*, MSL-mediated compensation, like early dosage compensation, is also non-uniform (Hamada *et al.* 2005). In humans, a total of 25% of X-linked genes escape or show variable patterns of inactivation (Carrel and Willard 2005), and, as in *Drosophila*, canonical dosage compensation is inactive early in embryonic development (Steele 1970). Incomplete dosage compensation also arises during the evolution of neo-X chromosomes, and in ZW sex-determination systems, such as birds, global dosage compensation is replaced by a variable system of tissue-specific compensation of individual genes (Mank

and Ellegren 2009). Phenotypic robustness is achieved not only through intrinsic or emergent mechanisms acting in gene networks (Manu *et al.* 2009; Acar *et al.* 2010) but also through specific adaptations involving individual genes, as exemplified by the ubiquity of microRNAs and redundant enhancers (Li *et al.* 2009; Frankel *et al.* 2010; Perry *et al.* 2010). Buffering of incomplete dosage compensation is likewise expected to be target-specific and therefore common, but subject to continual adaptive pressure to track changes in the efficacy of dosage compensation of continually evolving X-linked genes.

Acknowledgments

We thank J. Jaeger for providing MATLAB segmentation code; S. Wang, C. Williams, and A. Victorsen for technical assistance; J. Gavin-Smith for comments on the manuscript; and C. Miles, B. He, S. Lott, A. B. Carvalho, and K. P. White for discussion. This work was supported by award no. 1R01GM078381 (M.Z.L. and M.K.) from the National Institutes of Health and grant no. 5P50GM081892 from the National Institute of General Medical Sciences.

Literature Cited

- Acar, M., B. F. Pando, F. H. Arnold, M. B. Elowitz, and A. Van Oudenaarden, 2010 A general mechanism for network-dosage compensation in gene circuits. *Science* 329: 1656–1660.
- Akam, M., 1987 The molecular basis for metameric pattern in the *Drosophila* embryo. *Development* 101: 1–22.
- Baker, N. E., 1987 Molecular cloning of sequences from *wingless*, a segment polarity gene in *Drosophila*: the spatial distribution of a transcript in embryos. *EMBO J.* 6: 1765–1774.
- Belote, J. M., and J. C. Lucchesi, 1980 Control of X chromosome transcription by the *maleless* gene in *Drosophila*. *Nature* 285: 573–575.
- Carrel, L., and H. F. Willard, 2005 X-inactivation profile reveals extensive variability in X-linked gene expression in females. *Nature* 434: 400–404.
- Cline, T. W., 2005 Reflections on a path to sexual commitment. *Genetics* 169: 1179–1185.
- Dunipace, L., A. Ozdemir, and A. Stathopoulos, 2011 Complex interactions between *cis*-regulatory modules in native conformation are critical for *Drosophila snail* expression. *Development* 138: 4075–4084.
- Erickson, J. W., and T. W. Cline, 1993 A bZIP protein, *sisterless-a*, collaborates with bHLH transcription factors early in *Drosophila* development to determine sex. *Genes Dev.* 7: 1688–1702.
- Fowlkes, C. C., C. L. L. Hendriks, S. V. E. Keränen, G. H. Weber, O. Rübél *et al.*, 2008 A quantitative spatiotemporal atlas of gene expression in the *Drosophila* blastoderm. *Cell* 133: 364–374.
- Franke, A., A. Dernburg, G. J. Bashaw, and B. S. Baker, 1996 Evidence that MSL-mediated dosage compensation in *Drosophila* begins at blastoderm. *Development* 122: 2751–2760.
- Frankel, N., G. K. Davis, D. Vargas, S. Wang, F. Payre *et al.*, 2010 Phenotypic robustness conferred by apparently redundant transcriptional enhancers. *Nature* 466: 490–493.
- Frasch, M., and M. Levine, 1987 Complementary patterns of *even-skipped* and *fushi tarazu* expression involve their differential regulation by a common set of segmentation genes in *Drosophila*. *Genes Dev.* 1: 981–995.
- Frasch, M., T. Hoey, C. Rushlow, H. J. Doyle, and M. Levine, 1987 Characterization and localization of the *even-skipped* protein of *Drosophila*. *EMBO J.* 6: 749–759.
- Fujioka, M., J. B. Jaynes, and T. Goto, 1995 Early *even-skipped* stripes act as morphogenetic gradients at the single cell level to establish *engrailed* expression. *Development* 121: 4371–4382.
- Fujioka, M., Y. Emi-Sarker, G. L. Yusibova, T. Goto, and J. B. Jaynes, 1999 Analysis of an *even-skipped* rescue transgene reveals both composite and discrete neuronal and early blastoderm enhancers, and multi-stripe positioning by gap gene repressor gradients. *Development* 126: 2527–2538.
- Fujioka, M., G. L. Yusibova, N. H. Patel, S. J. Brown, and J. B. Jaynes, 2002 The repressor activity of *Even-skipped* is highly conserved, and is sufficient to activate *engrailed* and to regulate both the spacing and stability of parasegment boundaries. *Development* 129: 4411–4421.
- Gelbart, M. E., and M. I. Kuroda, 2009 *Drosophila* dosage compensation: a complex voyage to the X chromosome. *Development* 136: 1399–1410.
- Gergen, J. P., 1987 Dosage compensation in *Drosophila*: evidence that *daughterless* and *Sex-lethal* control X chromosome activity at the blastoderm stage of embryogenesis. *Genetics* 117: 477–485.
- Hamada, F. N., P. J. Park, P. R. Gordadze, and M. I. Kuroda, 2005 Global regulation of X chromosomal genes by the MSL complex in *Drosophila melanogaster*. *Genes Dev.* 19: 2289–2294.
- Harding, K., T. Hoey, R. Warrior, and M. Levine, 1989 Autoregulatory and gap gene response elements of the *even-skipped* promoter of *Drosophila*. *EMBO J.* 8: 1205–1212.
- Holloway, D. M., L. G. Harrison, D. Kosman, C. E. Vanario-Alonso, and A. V. Spirov, 2006 Analysis of pattern precision shows that *Drosophila* segmentation develops substantial independence from gradients of maternal gene products. *Dev. Dyn.* 235: 2949–2960.
- Ingham, P. W., A. Martinez-Arias, P. A. Lawrence, and K. R. Howard, 1985 Expression of *engrailed* in the parasegment of *Drosophila*. *Nature* 317: 634–636.
- Jaeger, J., 2011 The gap gene network. *Cell. Mol. Life Sci.* 68: 243–274.
- Janssens, H., D. Kosman, C. E. Vanario-Alonso, J. Jaeger, M. Samsonova *et al.*, 2005 A high-throughput method for quantifying gene expression data from early *Drosophila* embryos. *Dev. Genes Evol.* 215: 374–381.
- Kelley, R. L., I. Solovyeva, L. M. Lyman, R. Richman, V. Solovyev *et al.*, 1995 Expression of *msh-2* causes assembly of dosage compensation regulators on the X chromosomes and female lethality in *Drosophila*. *Cell* 81: 867–877.
- Larschan, E., E. P. Bishop, P. V. Kharchenko, L. J. Core, J. T. Lis *et al.*, 2011 X chromosome dosage compensation via enhanced transcriptional elongation in *Drosophila*. *Nature* 471: 115–118.
- Li, X., J. J. Cassidy, C. A. Reinke, S. Fischboeck, and R. W. Carthew, 2009 A microRNA imparts robustness against environmental fluctuation during development. *Cell* 137: 273–282.
- Lott, S. E., M. Kreitman, A. Palsson, E. Alekseeva, and M. Z. Ludwig, 2007 Canalization of segmentation and its evolution in *Drosophila*. *Proc. Natl. Acad. Sci. USA* 104: 10926–10931.
- Lott, S. E., J. E. Villalta, G. P. Schroth, S. Luo, L. A. Tonkin *et al.*, 2011 Noncanonical compensation of zygotic X transcription in early *Drosophila melanogaster* development revealed through single-embryo RNA-Seq. *PLoS Biol.* 9: e1000590.
- Lucchetta, E. M., J. H. Lee, L. A. Fu, N. H. Patel, and R. F. Ismagilov, 2005 Dynamics of *Drosophila* embryonic patterning network perturbed in space and time using microfluidics. *Nature* 434: 1134–1138.
- Ludwig, M. Z., A. Palsson, E. Alekseeva, C. M. Bergman, J. Nathan *et al.*, 2005 Functional evolution of a *cis*-regulatory module. *PLoS Biol.* 3: e93.

- Ludwig, M. Z., Manu, R., Kittler, K. P., White, and M. Kreitman, 2011 Consequences of eukaryotic enhancer architecture for gene expression dynamics, development, and fitness. *PLoS Genet.* 7(11): e1002364.
- Macdonald, P. M., P. Ingham, and G. Struhl, 1986 Isolation, structure, and expression of *even-skipped*: a second pair-rule gene of *Drosophila* containing a homeo box. *Cell* 47: 721–734.
- Mank, J. E., and H. Ellegren, 2009 All dosage compensation is local: gene-by-gene regulation of sex-biased expression on the chicken Z chromosome. *Heredity* 102: 312–320.
- Manu, S., Surkova, A. V., Spirov, V., Gursky, H., Janssens *et al.*, 2009 Canalization of gene expression in the *Drosophila* blastoderm by gap gene cross regulation. *PLoS Biol.* 7: e1000049.
- Markstein, M., C. Pitsouli, C. Villalta, S. E. Celniker, and N. Perrimon, 2008 Exploiting position effects and the gypsy retrovirus insulator to engineer precisely expressed transgenes. *Nat. Genet.* 40: 476–483.
- Mukherjee, A. S., and W. Beermann, 1965 Synthesis of ribonucleic acid by the X-chromosomes of *Drosophila melanogaster* and the problem of dosage compensation. *Nature* 207: 785–786.
- Perry, M. W., A. N. Boettiger, J. P. Bothma, and M. Levine, 2010 Shadow enhancers foster robustness of *Drosophila* gastrulation. *Curr. Biol.* 20: 1562–1567.
- Perry, M. W., A. N. Boettiger, and M. Levine, 2011 Multiple enhancers ensure precision of gap gene-expression patterns in the *Drosophila* embryo. *Proc. Natl. Acad. Sci. USA* 108: 13570–13575.
- Pritchard, D. K., and G. Schubiger, 1996 Activation of transcription in *Drosophila* embryos is a gradual process mediated by the nucleocytoplasmic ratio. *Genes Dev.* 10: 1131–1142.
- Rastelli, L., R. Richman, and M. I. Kuroda, 1995 The dosage compensation regulators MLE, MSL-1 and MSL-2 are interdependent since early embryogenesis in *Drosophila*. *Mech. Dev.* 53: 223–233.
- Schroeder, M. D., M. Pearce, J. Fak, H. Fan, U. Unnerstall *et al.*, 2004 Transcriptional control in the segmentation gene network of *Drosophila*. *PLoS Biol.* 2: E271.
- Small, S., R. Kraut, T. Hoey, R. Warrior, and M. Levine, 1991 Transcriptional regulation of a pair-rule stripe in *Drosophila*. *Genes Dev.* 5: 827–839.
- Small, S., A. Blair, and M. Levine, 1992 Regulation of *even-skipped* stripe 2 in the *Drosophila* embryo. *EMBO J.* 11: 4047–4057.
- Stanojevic, D., T. Hoey, and M. Levine, 1989 Sequence-specific DNA-binding activities of the gap proteins encoded by *hunchback* and *Krüppel* in *Drosophila*. *Nature* 341: 331–335.
- Stanojevic, D., S. Small, and M. Levine, 1991 Regulation of a segmentation stripe by overlapping activators and repressors in the *Drosophila* embryo. *Science* 254: 1385–1387.
- Steele, M. W., 1970 Incomplete dosage compensation for *glucose-6-phosphate dehydrogenase* in human embryos and newborns. *Nature* 227: 496–498.
- Straub, T., G. D. Gilfillan, V. K. Maier, and P. B. Becker, 2005 The *Drosophila* MSL complex activates the transcription of target genes. *Genes Dev.* 19: 2284–2288.
- Surkova, S., D. Kosman, K. Kozlov, and E. Manu Myasnikova *et al.*, 2008 Characterization of the *Drosophila* segment determination morphome. *Dev. Biol.* 313: 844–862.

Communicating editor: T. Schüpbach

GENETICS

Supporting Information

www.genetics.org/lookup/suppl/doi:10.1534/genetics.112.148205/-/DC1

Sex-Specific Pattern Formation During Early *Drosophila* Development

Manu, Michael Z. Ludwig, and Martin Kreitman

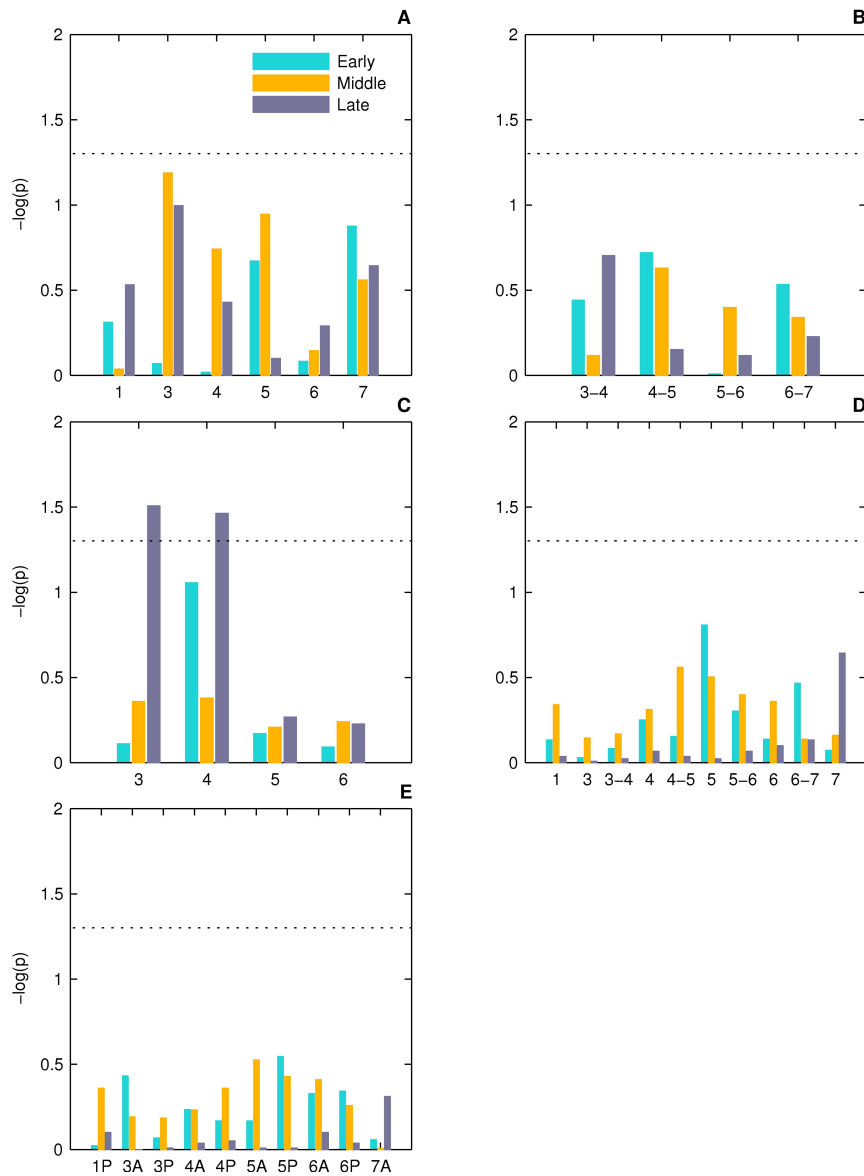


Figure S1 Statistical tests for sex-bias in the expression features of stripes 1, 3-7 in w^{1118} . p -values of Wilcoxon ranksum test between males and females for features of stripes 1, 3-7 are plotted as negative logarithms to base 10. Dotted line is at $p=0.05$. **A**, Peak expression; labeled with stripe number. **B**, interstripe expression; n-m is the interstripe between stripes n and m. **C**, relative repression; calculated as the ratio of the heights of anterior and posterior borders as in Fig. 1. **D**, positions of extrema; labeled with stripe number for peaks and the interstripe number for troughs. **E**, positions of borders; labeled with stripe number and either "A" or "P" for anterior or posterior borders respectively. Peak expression is the fluorescence at the peak of a stripe.

Interstripe expression is the fluorescence at the trough between two stripes. Peak and interstripe expression were normalized to mean fluorescence in each embryo. Only relative repression of stripe 3 and 4 (panel C) show sex bias. Sample size is the same as Fig. 1E.

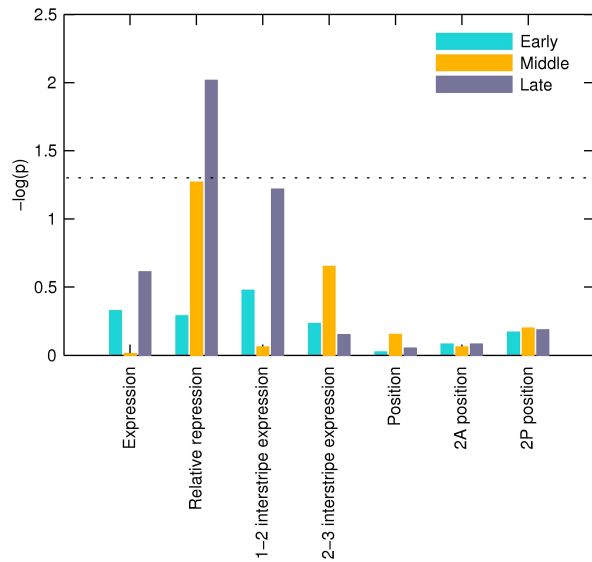


Figure S2 Relative repression is the only sex-biased stripe 2 feature in w^{1118} . The negative logarithm to base 10 of p -values of the Wilcoxon ranksum test between males and females. Dotted line is at $p=0.05$. Expression is the fluorescence at stripe peak. Relative repression is defined in Fig. 1. Interstripe expression is the fluorescence at the troughs between stripes 1 and 2 (1-2) and 2 and 3 (2-3). Peak and interstripe expression were normalized to mean fluorescence in each embryo. Position is the position of stripe 2 peak. 2A and 2P positions are the positions of the anterior and posterior borders respectively. Sample size is the same as Fig. 1E.

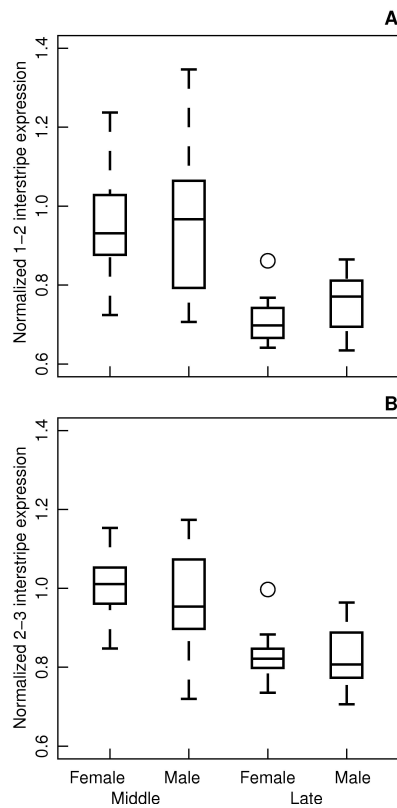


Figure S3 Interstripe 1-2 expression is elevated in w^{1118} males. Boxplots show normalized Eve expression in the 1-2 (A) and 2-3 (B) interstripes. See legend of Fig. 1 for an explanation of boxplot. Note that *greater* expression in an interstripe implies less repression, that is, *lower* values of relative repression. Sample size is the same as Fig. 1E.

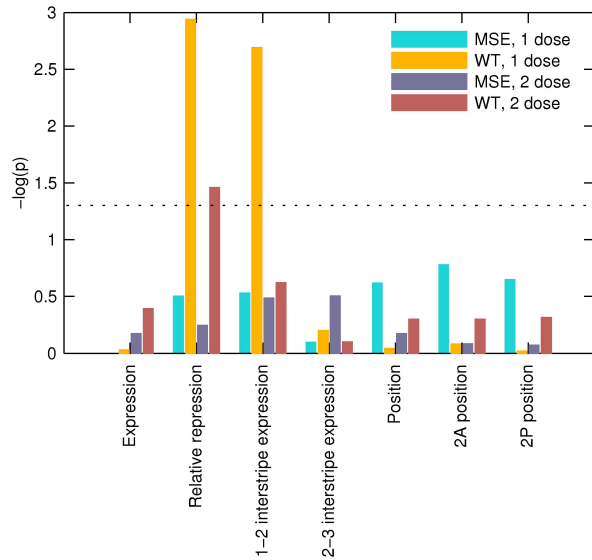


Figure S4 Relative repression is the only sex-biased stripe 2 feature in WT, while MSE lacks sex bias in all stripe 2 features. The negative logarithm to base 10 of p -values of the Wilcoxon ranksum test between males and females. Dotted line is at $p=0.05$. Expression is the fluorescence at stripe peak. Relative repression is defined in Fig. 1. Interstripe expression is the fluorescence at the troughs between stripes 1 and 2 (1-2) and 2 and 3 (2-3). Peak and interstripe expression were normalized to mean fluorescence in each embryo. Position is the position of stripe 2 peak. 2A and 2P positions are the positions of the anterior and posterior borders respectively. Sample size is the same as Fig. 2.

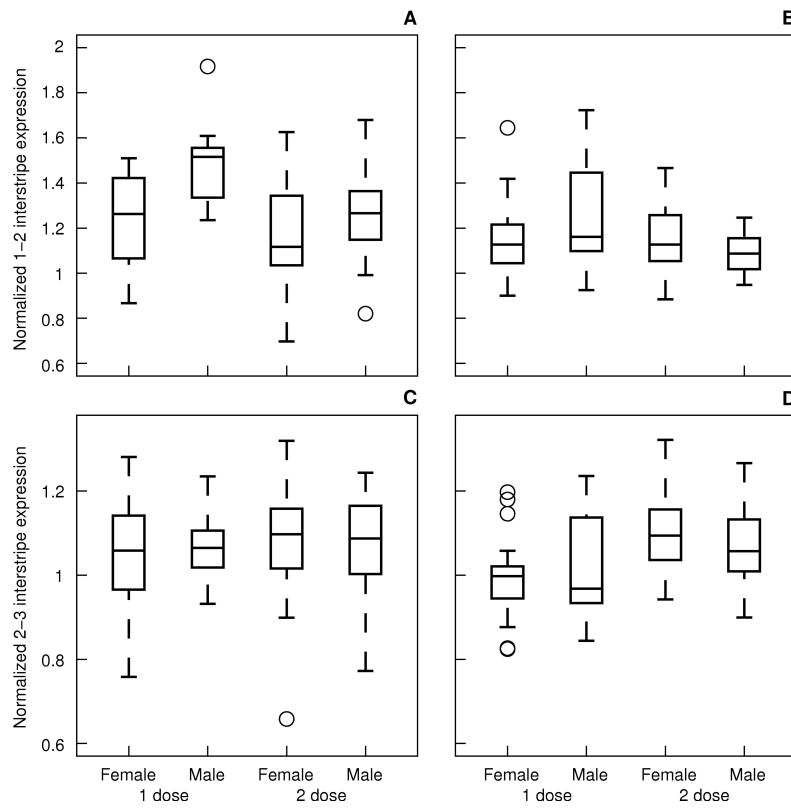


Figure S5 Interstripe 1-2 expression is elevated in WT, but not MSE males. Plots show normalized Eve expression driven by the WT or MSE transgenes in the 1-2 (**A,B**) and 2-3 (**C,D**) interstripes. See legend of Fig. 1 for an explanation of boxplot. **A,C**, WT. **B,D**, MSE. Note that *greater* expression in an interstripe implies less repression, that is, *lower* values of relative repression. Sample size is the same as Fig. 2.

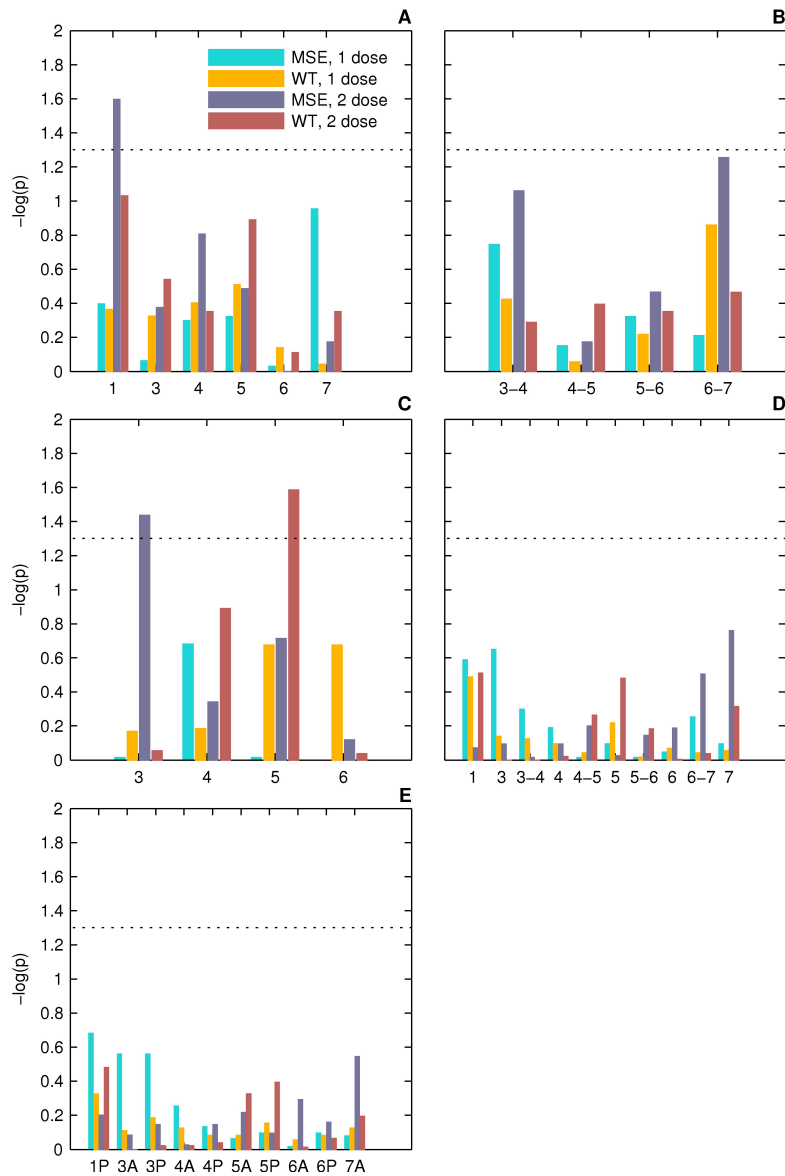


Figure S6 Statistical tests for sex-bias in the expression features of stripes 1, 3-7 when Eve expression is driven by WT or MSE. p -values of Wilcoxon ranksum test between males and females for features of stripes 1, 3-7 plotted as negative logarithms to base 10. Dotted line is at $p=0.05$. **A**, Peak expression, **B**, interstripe expression, **C**, relative repression, **D**, positions of extrema, and **E**, positions of borders. See Fig. S1 for an explanation of these phenotypes. Sample size is the same as Fig. 2.

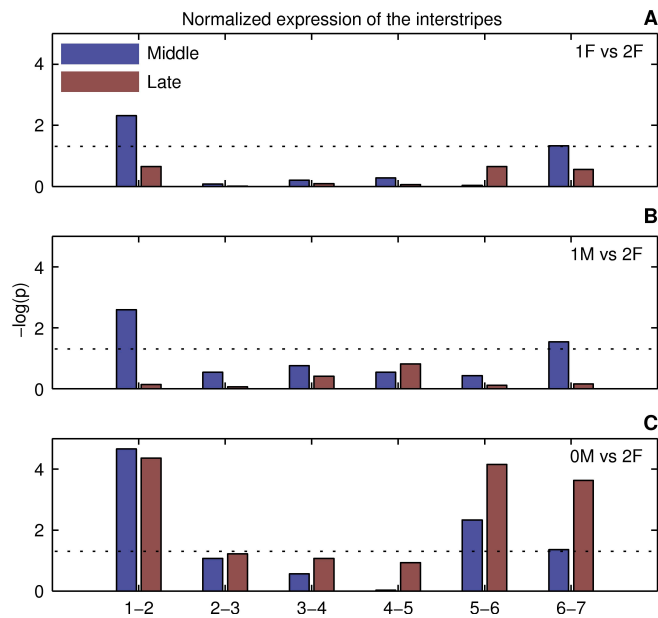


Figure S7 *gt* dose affects expression at the 5-6 and 6-7 interstripes. p -values of the Wilcoxon ranksum test on normalized interstripe expression between 1F (A), 1M (B), or 0M (C) and 2F genotypes are plotted as negative logarithms. Dotted line corresponds to $p=0.05$. Both 1M and 1F have the same pattern of differential expression, differing from 2F in the 1-2 and 6-7 interstripes but not elsewhere. 0M (*gt*) also differs from 2F in the same pattern except that 5-6 interstripe expression is also affected. Sample size is the same as Fig. 3B.

File S1

Supplementary Materials and Methods

Sequence of SYFP2 (*Drosophila* codon usage adjusted)

ATGGTGAGCAAGGGCGAGGAGCTGTTACCGGCGTGGTGCCCATCTGGTCGAGCTGGACGGCGACGTGAACGGCCACAAGTTCAGCGTGC
GCGGCGAGGGCGAGGGCGACGCCACCAACGGCAAGCTGACCCTGAAGCTGATCTGCACCACCGCAAGCTGCCGTGCCCTGGCCACCCT
CGTGACCACCCTGGGCTACGGCGTGCAGTGCTTCGCCCCTACCCCGACCACATGAAGCAGCAGACTTCTTCAAGTCCGCCATGCCCGAGGG
CTACGTCCAGGAGCGCACCATCTTCTCAAGGACGACGGCACCTACAAGACCCGCGCCGAGGTGAAGTTCGAGGGCGACACCCTGGTGAACC
GCATCGAGCTGAAGGGCATCGACTTCAAGGAGGACGGCAACATCCTGGGCCACAAGCTGGAGTACAACCTCAACAGCCACAACGTCTACATC
ACCGCCGACAAGCAGAAGAACGGCATCAAGGCCAACTTCAAGATCCGCCACAACGTGGAGGACGGCGGCGTGCAGCTCGCCGACCACTACC
AGCAGAACACCCCATCGGCGACGGCCCCGTGCTGCTGCCGACAACCACTACCTGAGCTACCAGTCCAAGCTGAGCAAGGACCCCAACGAG
AAGCGCGACCACATGGTCTGCTGGAGTTCGTGACCGCCCGCCGCATCACCCACGGCATGGACGAGCTGTACAAGTAA

Sequence of genomic *giant* 26149bp

Drosophila melanogaster Reference Sequence Release 5.30

Start X: 2312831

End X: 2338979

Primers for recombineering

***gt* –YFP fusion**

Primer_gtCYFP_F:

CCCTCAAGGTCCAGCTGGCCGCTTACCTCCGCCAAAGTAACCACCGCCGATTATGATATTCCAACACTACTGCAAGCATGGTGAGCAAGGGCG
AG

Primer_gtCYFP_R:

ACATACGATTCGGATCCTCGCGTTCAACGCATCAAGAGAGGAGTGGACCTTACTTGTACAGCTCGTCCATGC

For cloning from BAC to attB_3xP3_DsRed_P15A-amp

gt_intF2:

TATCTCAATAATACACATCTAGTTTCGGATCCTTAAGTCTACTTGAAACTCAGGCATTCAAATATGTATCC

gt_intR2:

CGTCATAAATGGCAGTGTCTTAAATTACAATCCTTCCCTTGGTCTTCTCGTCGACGATGTAGGTCACG

For verification of the insertion of the vector attB into attP2 landing site

See Ludwig *et al.* (2011).

Primers for genotyping

***p[hb-lacZ]* marker (800bp) for balancer second chromosome**

Z353 CTGCCAGTTTGAGGGGACGACGACA

hb32 ACCAACGTAATCCCATAGAAAA

Positive marker (80bp) of PCR genotyping reaction

sna-F CCCACGTGGACGTCAAGAA

sna-R GAGCGACATCCTGGAGAAAGA

Male fertility factor *k15* gene on the Y chromosome (240bp)

y6527 GGCCTAATTGGAGACCTGTTTC

y6749 CTGGTTTTGGTATGTCTTGTTA

p[GAL4-Kr.C] > p[UAS-GFP.S65T] on the X chromosome (600bp)

Pry1 CCTTAGCATGTCCGTGGGGTTTGAAT

5542GFP TTGCATCACCTTCACCCTCTCCCCT

Table S1 Mutant genotypes

Name	Description
<i>w</i> ¹¹¹⁸	<i>white</i> ⁻
WT	attP2[S2E ^{wt} EVE ^{YFP}] 16.4kb <i>eve</i> locus with wild type stripe 2 enhancer (S2E) and a YFP tag at the C-terminus of the <i>eve</i> coding region, integrated on the third chromosome
MSE	attP2[S2E ^{MSE} EVE ^{YFP}] 16.4kb <i>eve</i> locus with 244bp deleted from S2E (Fig. 2A) and a YFP tag at the C-terminus of the <i>eve</i> coding region, integrated on the third chromosome
<i>eve</i> ^{R13}	Null allele carrying a coding point mutation
<i>gt</i> ^{X11}	Null allele
<i>gt</i> ^{YFP}	attP2[GT ^{YFP}] 26.2kb region of the <i>gt</i> locus with a YFP tag at the C-terminus of the <i>gt</i> coding region, integrated on the third chromosome
<i>eve</i> ^{ΔMSE}	Native locus in which the MSE region of the stripe 2 enhancer is deleted and replaced with <i>w</i> ⁺ sequence (Ludwig <i>et al.</i> , 2005)

Table S2 Rescue of gt^{X11} by the gt^{YFP} transgene

Genotype [†]	Sex	<i>gt</i> copies	Number of enclosed adults
$gt^{X11}/+;gt^{YFP}/+$	FEMALE	1 endogenous + 1 transgene	623
$FM7c/+;gt^{YFP}/+$	FEMALE	2 endogenous + 1 transgene	535
$FM7c/Y;gt^{YFP}/+$	MALE	1 endogenous + 1 transgene	352
$gt^{X11}/Y;gt^{YFP}/+$ ^{††}	MALE	0 endogenous + 1 transgene	261

[†] Offspring of a cross between 8 $gt^{X11}/FM7c$ females and 8 gt^{YFP} males at 25°, scored as described previously (Ludwig et al., 2011).

^{††} The rescue potency of gt^{YFP} is estimated to be ~40% as the ratio between the number of adults of the $gt^{X11}/Y;gt^{YFP}/+$ and $gt^{X11}/+;gt^{YFP}/+$ genotypes. The rescued males were healthy and fertile.